JTTEE5 13:229-238
DOI: 10.1361/10599630418158
1059-9630/$19.00 © ASM International

Transient Contact Pressure During Flattening of Thermal Spray Droplet and Its Effect on Splat Formation

Chang-Jiu Li and Jing-Long Li

(Submitted 12 October 2002; in revised form 9 February 2003)

The flattening process of an isothermal droplet impinging on flat substrate in plasma spraying is studied numerically using "Marker-And-Cell" technique that enables the evolution of the droplet/substrate dynamic contact pressure. The distributions of the pressures upon substrate surface during flattening are calculated under different droplet conditions. The correlation of the distribution of the peak contact pressure along substrate surface with the observed splat morphology is examined. The results show that the transient contact pressure is initially high and concentrates at a small contacting area and then spreads quickly with droplet flattening. The maximum pressure is located at the front of the droplet at an early stage of deformation, which drives the fluid moving quickly along substrate and results in lateral flow. The contact pressure is mainly associated to droplet density and velocity. The peak pressure reduces monotonically with flattening and becomes negligible at the region where the flattening degree is larger than 2. The magnitude of the pressure resulting from evaporating gas by rapid heating of the adsorbed water on the substrate surface is comparable to that of the dynamic contact pressure at the region where the flattening degree ranges from 1.5 to 2. It is suggested that the reduced contact pressure at the late stage of spreading and disturbance by the evaporation-induced pressure resulting from rapid heating of the surface adsorbents by flattening droplet may contribute significantly to the splashing of flattening droplet and the formation of a reduced disk-like splat.

Keywords droplet impact, dynamic contact pressure, flattening, numerical simulation, plasma spray, splashing, splat formation

1. Introduction

A thermal spray coating is built up by a stream of molten droplets. The individual droplet forms a splat through processes of impacting, flattening, rapid cooling, and solidification. The analysis has clearly revealed that the deposition of an individual splat in the coating can be considered as an independent event, which is not significantly influenced by the deposition of other splats.[1] Consequently, individual single splat formation has a significant effect on the coating structure and property and the adhesion of a coating to substrate and is one of the most fundamental topics concerning formation of sprayed coating. Therefore, many studies have been done on splat formation. The studies were experimental[2-7] and theoretical.[8-11]

The experimental examination of splat morphology has led to the progressive understanding of the phenomena related to its formation. It is known that the splashing will occur when a droplet impacts at ambient atmosphere even on a flat surface. However, when substrate is preheated up to about 200 °C, the splashing will be suppressed.[4-6] The splashing is closely associated with the interaction of impacting droplet with a substrate.

Chang-Jiu Li, State Key Laboratory for Mechanical Behavior of Materials, School of Materials Science and Engineering, Xi'an Jiaotong University, Xi'an, Shaanxi, 710049, People's Republic of China; and **Jing-Long Li,** College of Materials Science and Engineering, Northwestern Polytechnological University, Xi'an, Shaanxi, People's Republic of China. Contact e-mail: licj@mail.xjtu.edu.cn.

Nomenclature

C_0	constant for initial contact pressure
C_s	velocity of the sound in liquid, m s^{-1}
d	diameter of spherical droplet, m
D	diameter of splat, m
f	body force
p	scalar pressure, N m^{-2}
P_0	water-hammer pressure, N m^{-2}
r	radius of curvature of the droplet, m
Re	reynolds number, $\rho\, dw_0/\mu$
t	time, s
V	velocity vector
w_0	droplet velocity, m s^{-1}
y	radial coordinate representing the diameter of splat, m
z	vertically symmetrical coordinate representing the height of splat, m
α	factor to the water hammer pressure
μ	viscosity, N m^{-2} s
ρ	density, kg m^{-3}
σ	surface tension, N m^{-1}
τ	dimensionless time, $t\, w_0 /d$
ξ	dimensionless radial axis abscissa, $2y/d$
ξ_m	flattening degree, D/d
ζ	dimensionless symmetrical axis ordinate, z/d

On the other hand, it is difficult to examine experimentally the interactions between a thermal spray droplet and a substrate due to dynamic of flattening and solidification. In fact, these processes take only a few microseconds.[12] That is why numerical simulation became an important method in such investigation. The earlier numerical works were mainly concerned with the flattening process of droplet by relating the flattening degree to droplet parameters such as Reynolds Number and Weber number.[8-10] The approach has successfully exhibited the characteristics of flattening process to an ideal disk splat and illustrated that flattening degree predicted by commonly cited Madejski's model[13] over-estimates the flattening of droplet.[9] The recent numerical approach attempts also to involve the splashing based on the Rayleigh-Taylor instability theory.[11]

Based on the experimental results, the mechanism for the splashing, which takes place during flattening of spray molten droplet, have been proposed.[6,14] One mechanism, the evaporated-gas-induced splashing model, revealed the dominant effect of the gas formed through the evaporation of adsorbates on substrate surface. This effect has also been confirmed by Jiang et al.[15] The other mechanism, the surface-melting-induced splashing model, was proposed to explain the splashing, which occurs when the surface of the substrate is melted by impacting droplet.[6,7] It was also argued that the splashing might result from a localized solidification.[16] Despite the different models, the common point of the models mentioned above is that the direction of flattening fluid determined by its inertia force cannot follow closely to substrate surface due to the discontinuity of surface backing the fluid or the additional force resulting from the evaporated gas between fluid and substrate. Those effects tend to detach the fluid from substrate surface. This implies that, on the other hand, the mechanical conditions resulting from both droplet deformation process and substrate surface conditions will be essentially important with regards to the splashing. When the contact pressure between spreading droplet and substrate surface is large enough to keep liquid to contact closely with substrate, the splashing may not occur. Therefore, it can be considered that the dynamic pressure evolved in droplet fluid toward the substrate during flattening will significantly influence the droplet flattening behavior. However, there are few reports that have been concerned with the problem up to now except the work reported by Montavon et al.[17]

In this study, the spreading process of a droplet after impact is simulated numerically. The main emphasis is put on the systematical study into the distribution and change of the transient contact pressure of droplet to the substrate under different droplet conditions during the spreading process and the examination of the effect of the subsequent transient pressure on splat formation in thermal spraying.

2. Method of Calculation

The deformation motion of a molten droplet can be described by the incompressible Navier-Stokes equations. The governing equations include the continuity equation and the full Navier-Stokes equations for transient, axisymmetric, viscous, incompressible fluid flow in a Eulerian frame as follows:

$$\nabla \cdot \vec{V} = 0 \qquad \text{(Eq 1)}$$

$$\frac{\partial \vec{V}}{\partial t} + (\vec{V} \cdot \nabla)\vec{V} = -\frac{1}{\rho}\nabla p + \frac{\mu}{\rho}\nabla^2 \vec{V} + f \qquad \text{(Eq 2)}$$

where $\vec{V}$ is the vector velocity, t the time, ρ the fluid density, p the scalar pressure, μ the fluid viscosity, f the body force per unit density. The complete equations were solved on a Eulerian rectangular mesh in cylindrical geometry using a commercial PHOENICS Code (PHOENICS 1.4),[18] and "Marker-And-Cell" technique (MAC)[19] was used to trace the free surface and fluid domain of droplet during deformation. The calculation was performed under the isothermal conditions corresponding to different viscosity and surface tension. The details of the numerical scheme and solution techniques have been described in detail elsewhere.[20] Most of the results are normalized in the dimensionless forms as follows:

$\tau = tw_0/d$, dimensionless (inertial) time;

$\xi = 2y/d$, dimensionless abscissa (radial axis); the maximum value at a given time represents the relative radius (or diameter) of flattening droplet, i.e., the flattening degree;

$\zeta = z/d$, dimensionless ordinate (symmetrical axis) which represents the relative height of flattening droplet, i.e., the thickness of splat.

where w_0 and d are impact velocity and initial droplet diameter; y and z the abscissa dimension and ordinate dimension (thickness), respectively. The selected calculation conditions were w_0 = 25-400 m/s, d = 25-200 μm, ρ = 1-16 × 10^3 kg/m^3, μ = 2.5-20 × 10^{-3} Pa s and surface tension coefficient σ = 0-2 N/m. The computations took 2-6 h of computer time.

3. Simulation Results

3.1 Droplet Spreading Process

Figure 1 illustrates the evolution of the spreading process for a droplet of 100 μm in diameter with a density of 8 × 10^3 kg/m^3 that impacts on a flat substrate surface at a velocity of 100 m/s. It was found that the transverse flow along the substrate surface occurs first at the time of τ = 0.1-0.2 after impact. It spreads quickly along the surface with the falling of droplet height, which reaches the final splat diameter ξ_m (defined as flattening degree) and thickness ζ_m. ξ_m and ζ_m are influenced by droplet size, density, viscosity, and impact velocity, which can be normalized as the influence of the Reynolds number (Re) on the flattening degree, where Re = $\rho w_0 d/\mu$. With the increase in the Reynolds number, the splat diameter will be increased and the splat thickness will be decreased. Numerically, the estimated splat size ranged from 4.06-7.81 of ξ_m, and 0.013-0.044 of ζ_m at ρ = 2-8 × 10^3 kg/m^3, w_0 = 50-400 m/s, μ = 2.5-20 × 10^{-3} Pa s and d = 25-200 μm that cover most of the plasma spray conditions.

The examination into the relationship between the Reynolds number and the flattening degree obtained by numerically simulated results revealed that when the modification is made to Madejski's relation[13] the following equation fitted the data best.

$$\xi = 1.025\ \mathrm{Re}^{0.2} \qquad \text{(Eq 3)}$$

The comparison of the coefficient obtained in this study with those obtained by other investigators is shown in Table 1. There-

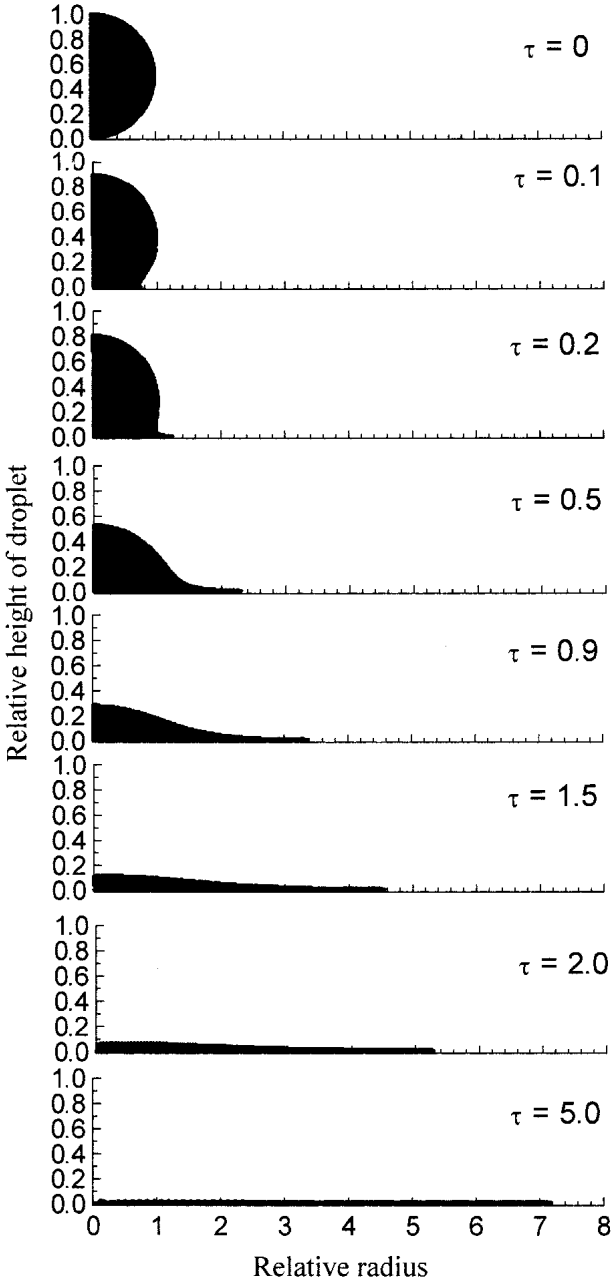

Fig. 1 Typical droplet flattening patterns at different times (w_0 = 100 m/s; d = 100 μm; ρ = 8 × 10^3 kg/m^3; μ = 5 × 10^{-3} Pa s; σ =1 N/m)

fore, this correlation gives a coefficient of 1.025 smaller than 1.2941 in Madejski's relation for the plot of ξ against $Re^{0.2}$. This coefficient is very close to that given by Trapaga et. al.[8] and to 1.04 by Liu et al.,[10] which was also obtained at the isothermal conditions, and larger than a modified coefficient of 0.925 proposed by Bertagnolli et al.[9] The later is obtained by taking the effect of solidification on flattening into the consideration during the simulation. Consequently, the above difference would be reasonable because the thermal reaction of droplet material with substrate may influence the flattening process. Such agreement of the simulated flattening degree with those reported proved the validity of the present simulating method, which was used to simulate the transient pressure during droplet flattening. Although all simulated results yielded a close coefficient value, it should be pointed out that the recent experiment under known velocity and temperature of the particles in a narrow size range yielded a significantly low coefficient.[21]

Table 1 Comparison of the Coefficient a for the Formula ξ = a $Re^{0.2}$ Obtained by Different Investigators

Coefficient	Investigators	Reference	Remark
1.249	Madejski	13	Theoretical model
1	Trapaga et al.	8	Simulated at isothermal conditions
1.04	Liu et al.	10	Simulated at isothermal conditions
0.925	Bertagnolli	9	Simulated by taking account of solidification effect
1.025	Present study		Simulated at isothermal conditions

3.2 Evolution of Contact Pressure

Figure 2 shows the evolutions of the transient pressure contours from τ = 0.004-0.5 under the conditions of ρ = 8 × 10^3 kg/m^3, w_0 = 100 m/s, μ = 5 × 10^{-3} Pa·s and d = 100 μm. The initial contact pressure at the impact, which is highest with a steep pressure gradient, is concentrated around a small contact area as shown at τ = 0.004 in Fig. 2. The pressure then spreads and releases quickly with the flattening of the droplet. The pressure gradient keeps highest at the front of fluid during a period of time after impact, as shown at τ = 0.004, 0.02, 0.06, 0.1, and 0.2 in Fig. 2, which accelerates the fluid front flowing along the substrate in a very high speed and forms a lateral spreading flow. The calculated results show that the maximum velocity of spreading flow is mainly related to the impact velocity and reaches $3w_0$, which is consistent with that reported by Trapaga et al.[8] The pressure inside the droplet is depleted gradually when the deformation of droplet further progresses as shown at τ = 0.2 and 0.5 in Fig. 2.

3.3 Initial Contact Pressure

The simulation showed that the contact pressure of droplet to substrate after impact is mainly dependent on the droplet density and impact velocity and the droplet viscosity has little effect on the initial contact pressure. Table 2 and 3 show the initial contact pressure obtained under different densities and impact velocities, respectively. The pressure at the very early flattening time, i.e., τ = 0.004, was changed with the droplet density and impact velocity, which ranged from several 10 MPa up to over 10^4 MPa. It increases with the droplet density and impact velocity. Furthermore, it was found from those results that the initial contact pressure p_0 increases linearly with droplet density ρ and square impact velocity w_0^2, i.e.,

$$p_0 = C_0 \rho w_0^2 \quad \text{(Eq 4)}$$

where the constant C = 3.75 in present study. This means that the initial impact pressure is about 7.5 times of stagnation pressure of the incompressible flow given by the Bernoulli equation.[22]

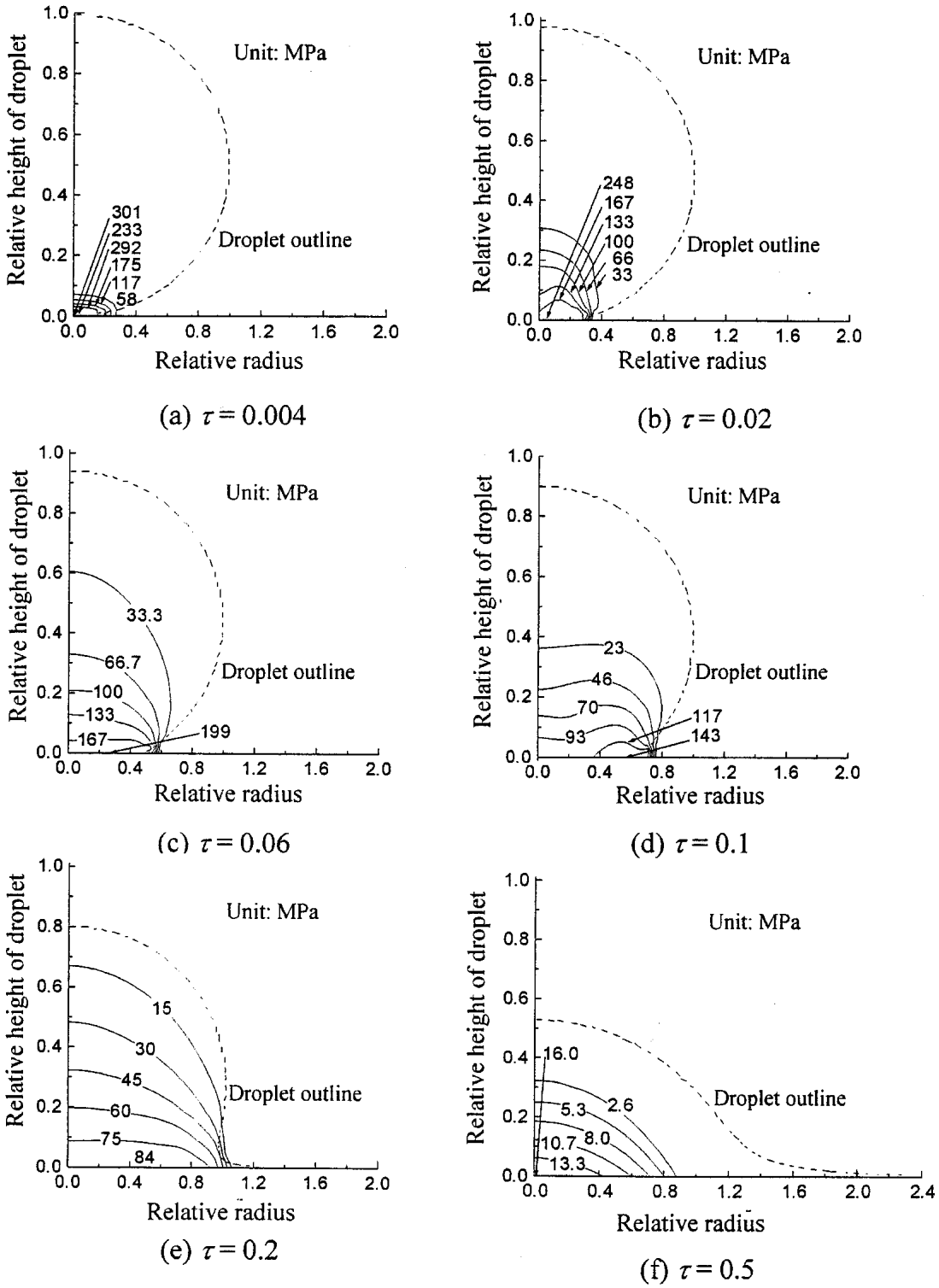

Fig. 2 Evolutions of transient pressure contours with flattening time (w_0 = 100 m/s, ρ = 8 × 10^3 kg/m^3)

With the impact pressure resulting from water drop-to-solid collisions, Engel[23] presented the following equation given by Honegger[24]:

$$p = 3.92 \times 10^3 w_0^2 \quad \text{(Eq 5)}$$

When one substitutes the density of water 1 × 10^3 kg/m^3 into Eq 4, then the initial contact pressure for water drop impact,

$$p = 3.75 \times 10^3 w_0^2 \quad \text{(Eq 6)}$$

Accordingly, it can be recognized that the present simulated result expressed by Eq 4 and 6 agrees well with that (Eq 5) given by Honegger.[24]

The high pressure resulting from initial impact will begin to release after a time.[25]

$$t_0' = \frac{3rw}{2C_s^2} \quad \text{(Eq 7)}$$

where C_s is the velocity of a compression wave in the liquid, r the radius of curvature of the droplet (liquid mass) in the region of contact. Comparing the corresponding real time to the dimensionless time $\tau = 0.004$ with that calculated by Eq 7, it can be found that the real time to obtain the initial contact pressure is less than that calculated by this equation within the simulating conditions in this study. Therefore, it can be considered that the initial contact pressure corresponds to the high pressure resulting from impact well before the pressure release commences.

When a liquid droplet impacts on a solid surface, the resulting maximum pressure under compressible condition is so-called water-hammer pressure.[26] For impact of cylindrical water jet on a rigid target, the pressure is

$$p_0 = \rho C_s w_0 \quad \text{(Eq 8)}$$

For the impact of a spherical water droplet, the following equation is valid[23]:

$$p_0 = \frac{1}{2}\alpha(\rho C_s w_0) \quad \text{(Eq 9)}$$

where α is a factor tending to unity at high velocities. Bowden and Tabor[27] measured experimentally the impact load of water jet with a core diameter of 1.3 mm and a head diameter of 3 mm striking the pressure gauge at an impact velocity of 720 m/s on using a piezoelectric pressure transducer. They obtained a peak load of 630 kg and gave an average pressure of 930 MPa by using the head diameter to illustrate the good agreement of this observed value with the theoretical value of 1058 MPa calculated for a water jet with an impact velocity of 720 m/s and C_s = 1500 m/s. However, when one considers the lateral flow of water jet at the early stage of impact to be restricted, it would be more reasonable to consider that the diameter of the effective area for impact load to act on is equal to the core diameter of water jet. Using the core diameter of water jet, one can obtain an impact pressure of 4740 MPa, which is about five times of that given by Bowden and Tabor.

For a spherical water droplet impacting at a velocity of 720 m/s, the theoretical pressure can be obtained to be 2133 MPa following Engel's approach with $\alpha = 0.9$.[23] With the velocity of 720 m/s, an initial contact pressure has a value of 1944 MPa, which was calculated according to Eq 6 obtained in this study. This value agrees well with that calculated by Eq 9. Therefore, the initial contact pressure expressed in Eq 4 obtained in this study would be valid to predict the maximum impact pressure although it was obtained under simulation condition of incompressible fluid.

3.4 Pressure Distribution Along Substrate Surface

The initial contact pressure only acts on the small surface area where the droplet just touched the substrate. Thus, to understand the interactions between droplet and substrate, it is necessary to examine the distribution and change of transient contact pressure throughout the process of droplet deformation. Figure 3 shows the distribution and change of the transient pres-

Table 2 Initial Dynamic Contact Pressure Simulated With Different Density Values

Density (kg m^{-3})	1000	2000	4000	8000	16 000
Pressure (MPa)	37.8	75.5	151.5	301.7	603.0

Note: w_0 = 100 m/s

Table 3 Initial Dynamic Contact Pressure Simulated at Different Droplet Velocity

Velocity (m · s^{-1})	25	50	100	200	400
Pressure (MPa)	18.8	75.5	301.7	1206.0	4825.0

Note: $\rho = 8 \times 10^3$ kg/m^3

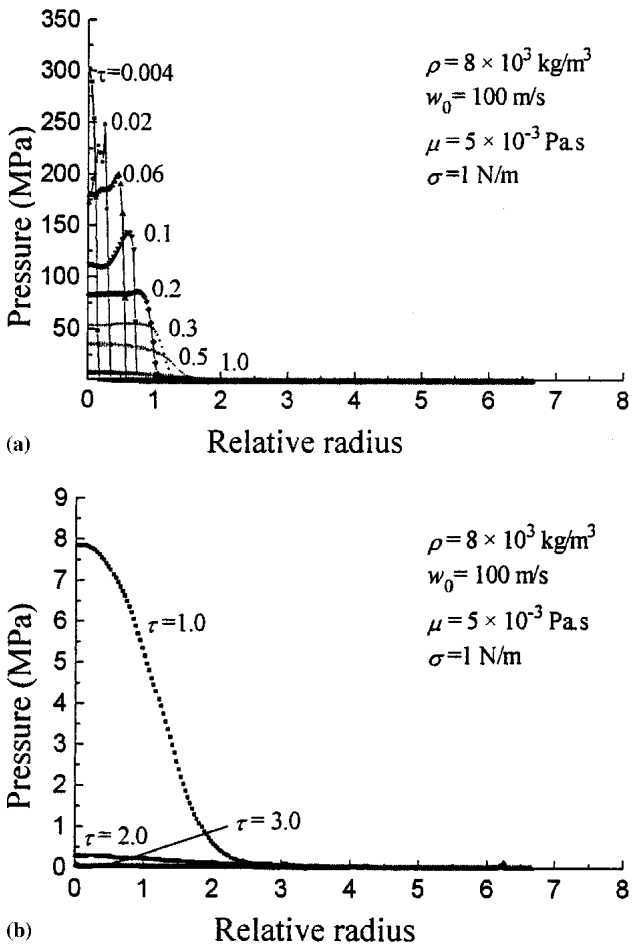

Fig. 3 Distributions of the dynamic contact pressure along substrate surface at different flattening times

sures along substrate surface with spreading time. Figure 3(b) shows the detailed indication of the pressures after τ becomes larger than 1. It can be found that at the early stage of the deformation at τ = 0-0.1, the pressure decays in a very high speed of more than 1500 MPa per unit dimensionless time. The maximum pressure and the maximum pressure gradient remain at the droplet front along surface, which cause the droplet to spread along surface at a very high speed. At the middle and later stages of the deformation, the pressures acted upon the substrate by the droplet become small and more uniform. It was also found (Fig. 3b) that during spreading, when the fluid front reached to an area of $\xi > 2$, the contact pressure at the front becomes less than 1 MPa. This implies that the contact pressures act effectively only within the area of $\xi < 2$, which is much less than the final splat diameter (4.06-7.81 in present study). On the other hand, at the area of $\xi > 2$, there is no effective pressure to keep the spreading fluid to contact closely with the substrate underneath. Such condition will make the spreading process of droplet material to be easily disturbed by substrate surface conditions.

3.5 Peak Pressure

The contact pressure generated by droplet impact assures the close contact between flattened droplet and substrate and consequently the effective contact between the splat and the substrate. According to the pressure distribution mentioned above, the contact pressure field changes continuously throughout the whole flattening process. However, the maximum pressure at a certain location is more important for the generation of good contact between fluid and the substrate. Therefore, the maximum pressure at a certain location of the substrate is defined as the peak pressure in the current study. The distributions of the maximum pressure along the substrate obtained at different droplet densities and impact velocities are shown in Fig. 4. The peak pressure increases with droplet density and impact velocity. Moreover, those results clearly show that the peak pressure is initially high in the center of droplet/substrate interface, and then decreases gradually along the surface. It drops to as little as less than 10 MPa at the location of ξ = 1.5 and below 1 MPa when the lateral flow of droplet reaches to and over ξ = 2 where the fluid of droplet, as shown in Fig. 1, moves mainly in the radial direction in a lower spreading velocity of about 0.8-1.6w_0. Therefore, the axial deformation velocity of droplet towards the substrate surface is too small at current time to give effective contact pressure upon substrate. The fluid of flattening droplet, while it passes over the region of $\xi > 2$, may mainly "float" upon substrate and it would be difficult for liquid to achieve the effective contact with substrate over this region, provided the ideal disk-like splat is formed. This can be considered to be the direct cause of incomplete contact at the interface between lamellae within coating.[28-30]

On the other hand, the numerically simulated results also revealed that the transient contact pressure at a given time step and a location of substrate also fit the equation given by Eq 4, where p_0 should be substituted by p, i.e., the transient contact pressure,

$$p = C(\tau,\xi)\rho w_0^2 \quad \text{(Eq 10)}$$

where the coefficient C ($C \le C_0$) is a function of time and distance of location. Equation 10 expresses the relationship between the contact pressure and the initial dynamic force of droplet. Figure 5 illustrates the simulated contact pressure at different times as a function of the location (ξ) and ρw_0^2. Therefore, the transient pressure depends on the kinetic energy of spray droplet. With the increase in the velocity and density of molten droplet material, the contact pressure will be increased.

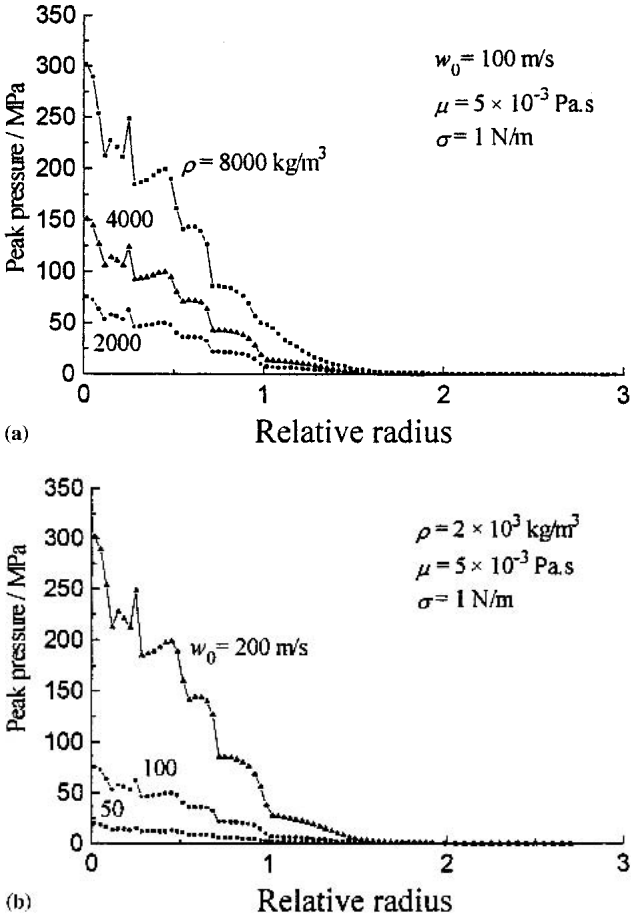

Fig. 4 Effect of **(a)** droplet density and **(b)** velocity on the peak pressure distributions along substrate surface

4. Effect of Contact Pressure on Splat Morphology

The splat morphologies have been systematically studied experimentally.[2,3,6,7,14,31] The splats were deposited on polished stainless steel substrate by plasma spraying in ambient atmosphere. The splat materials included copper (Cu), nickel (Ni), aluminum (Al), and molybdenum (Mo), which were sieved to a narrow size. The nominal particle size ranges were 76-90 μm for Cu and Mo, 75-64 μm for Ni, respectively. With Mo splat, Mo sheet with surface polished was used as substrate to avoid the melting of substrate surface by impacting molten droplet. With Cu and Ni splat formation was performed under different plasma arc powers. The experimental details were described elsewhere.[3] The morphology of the splat was examined using scanning electron microscopy (SEM). The size of splats was

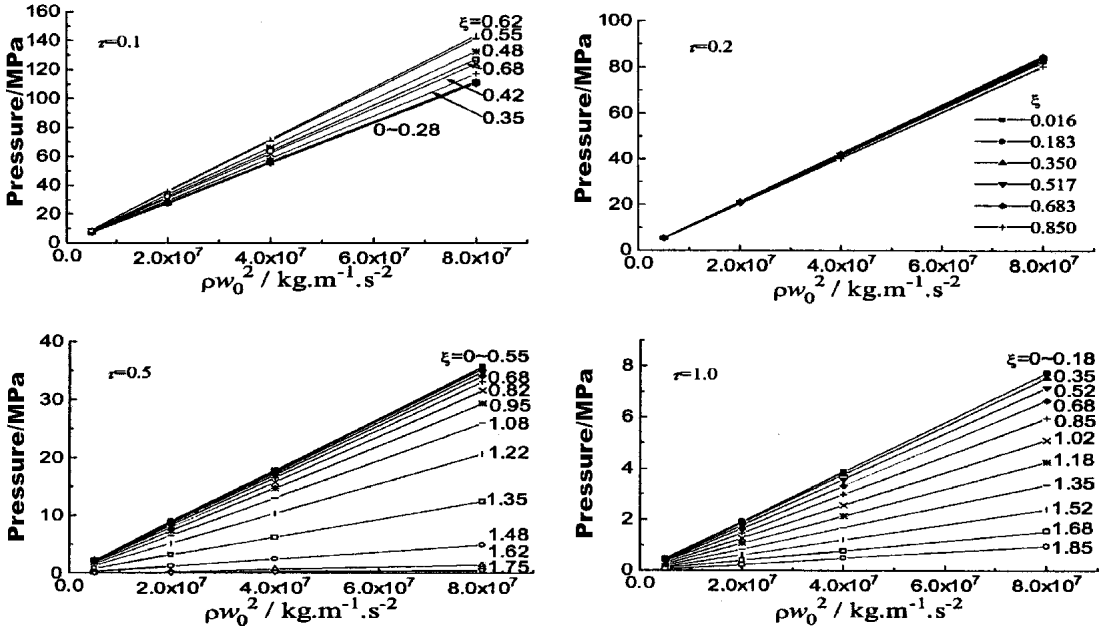

Fig. 5 Linear relationship between impact pressure and ρw_0^2 at different times from τ=0.1-1.0 and different positions

Table 4 Apparent Flattening Degrees of Cu Splats Obtained at Different Plasma Powers

Plasma power/kW	16 (400A-40V)	24 (400A-60V)	25 (500A-50V)	28 (400A-70V)	30 (500A-60V)
Apparent flattening degree	2.82	2.12	1.65	1.73	2.01

Table 5 Apparent Flattening Degrees of Ni Splats Obtained at Different Plasma Powers

Plasma power/kW	24 (400A-60V)	30 (500A-60V)	35 (700A-50V)	36 (600A-60V)	42 (700A-40V)
Apparent flattening degree	1.58	1.60	2.00	1.53	1.97

estimated from SEM photographs to obtain the apparent flattening degree of splats.

The experimental investigation has revealed that most splats formed on flat substrate by fully molten droplets in plasma spraying under ambient atmosphere were only a central part of an expected ideal disk-like one. Such reduced disk-like splat was defined as annulus ringed disk-like splat.[3,7] Figure 6 illustrates typical Ni splat deposited on flat stainless substrate surface along with thickness profile. The complete disk-like splat can be obtained only under very limited conditions such as on preheated flat surface[4-6] and/or at low particle impact velocity.[2] With the average powder grain size and the measurement of splat thickness as shown in Fig. 6(b), a flattening degree of about 5 is expected, which is consistent with the simulated results. Figure 7(a) and 7(b) illustrate typical Cu splat on flat stainless surface and Mo on molybdenum surface plasma-sprayed at ambient atmosphere, respectively. The splat of similar morphology was confirmed with other spray materials.

Table 4 and 5 summarize the apparent flattening degrees (ratio of splat diameter observed to particle size) for Cu and Ni splats obtained at different plasma powers on plasma spraying. Except one of Cu splat, which was deposited at a low plasma power of 16 kW and yielded a flattening degree, about 3 corresponding to complete disk-like splat as shown in Fig. 8, the apparent flattening degrees, ranged from 1.5 to 2, are much lower than that could be expected from average thickness of splats. This is because the present splat is only a central fraction of the expected complete disk-splat.

The formation of the reduced disk-like splat is associated with the occurrence of splashing during flattening of droplet. Based on the experimental results concerned with the effect of substrate temperature and evaporative organic substance adsorbed on substrate surface on splat formation, the evaporated gas induced splashing mechanism has been proposed.[6,14] According to this splashing mechanism, when a cold substrate is adsorbed by water from the moisture in the atmosphere, the adsorbent will be evaporated when the substrate surface is heated rapidly upon flattening of droplet. The resulting gas may be concentrated and tends to escape radially outwards, which will cause an upward force and subsequently upward fluid flow perpendicular to the direction of flattening.

Glod et al.[32] reported that under rapid heating the explosive evaporation of water on a surface from boiling occurs, which generates the excess pressure from 0.1 to 1MPa corresponding to a heating rate from 10^6 K/s to 8.6×10^7 K/s. They also showed that the force increases with the increase in heating rate. The flattening time of a spray droplet is usually less than about 2 μs[33] and surface temperature of the substrate resulting from the

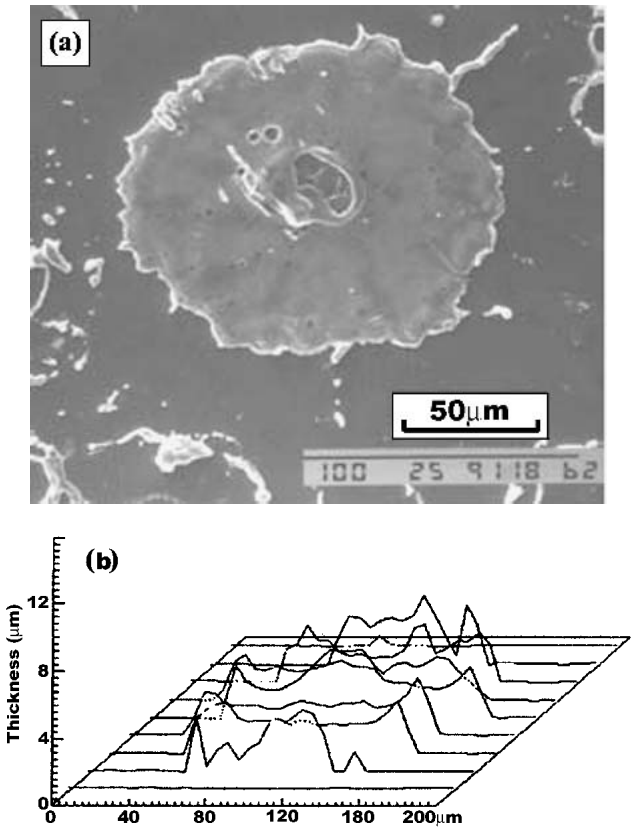

Fig. 6 **(a)** The morphology of a typical reduced Ni splat and **(b)** distribution of splat thickness

heating of the droplet can be raised to several hundreds degrees after a spray molten droplet impacts on a substrate. When materials with high melting points, such as refractory metal droplet molybdenum was used, the melting of steel substrate surface clearly indicated the rise of substrate temperature up to over 1000 °C heated by impacting droplet.[7,33] Therefore, the heating rate of the substrate surface by impacting droplet during spraying is of an order of about/over 10^8 K/s. This heating rate is coincident with those reported by Glod et al.[32] Park et al.[34] reported the pressure from the rapid vaporization of water on a surface generated by a pulsed-laser heating. They reported a pressure pulse of around 0.5 MPa at the bubble nucleation threshold to laser radiation energy. With the increase in radiation energy of laser pulse, the pressure generated increases to the order 1 MPa with a saturated level. The result reported by Park et al.[34] is the same in the order as those reported by Glod et al.[32]

Therefore, it can be considered that the force resulting from the evaporation of surface adsorbed water is of the same order as those of contact pressure at the region of splat ξ =1.5-2. Accordingly, comparing such excess pressure with the dynamic contact pressure of fluid on substrate resulted from the deformation of droplet, it is clear that at the region ξ = 1.5-2 the evaporated gas induced upward force may become comparable to the dynamic contact pressure. Moreover, beyond such a region, the excess force resulting from evaporated gas acts at the interface between fluid and substrate on spreading liquid through a gas cushion on the surface of the substrate. Due to the depletion of the dynamic contact pressure, the excess force resulted from evaporated gas tends to detach the spreading fluid from substrate and jet it away, i.e., splashing. As a result, the residual disk-like splat is formed.

As shown in Fig. 3, the contact pressure during droplet flattening concentrates within region $\xi < 1.5$. At the central area where droplet impact directly, the contact pressure may be as great as over 300 MPa at the initial flattening time steps. In this region, the evaporating gas may find no way to be released under such a high pressure. On the other hand, the evaporated gas may be absorbed by liquid droplet in much super-saturated state under high pressure. When the dynamic pressure is diminished under the evolution of shock wave in the liquid fluid, the absorbed gas might be condensed to form a gas bubble. This phenomenon could be a possible reason for the occurrence of central splashing observed previously,[2] as can be seen from splats in Fig. 6-8.

Although a quantitative model should be further developed to explain the coaction of impact dynamic pressure and evaporation-induced pressure, the present results evidently indicate that the contact pressure during droplet flattening influences significantly the occurrence of splashing during droplet flattening. It can be suggested that the reduced contact pressure at the late stage of spreading and disturbance by the evaporation-induced pressure resulting from rapid heating of the surface adsorbents by flattening droplet may contribute significantly to the splashing of flattening droplet and the formation of a reduced disk-like splat.

4. Conclusions

1) The maximum pressure gradient along the substrate concentrates at the front of droplet at early flattening stages, which accelerates the droplet spreading along substrate surface in a high velocity. The contact pressure spreads and dissipates quickly with the droplet flattening. The maximum spreading velocity reaches to 3 times of droplet velocity.
2) The contact pressure is increased proportionally to the droplet density and the square of impact velocity. The viscosity of the liquid shows little influence on the contact pressure. Though the peak pressure is initially high at the center of contact area of droplet with substrate, it consistently decreases along the substrate surface, which results in close contact between splat and substrate in a limited central area. Beyond this area, the fluid of droplet may float on the substrate surface with little effective contact pressure.
3) The transient contact pressure at a certain time step and location of substrate during droplet flattening process is linearly proportional to initial dynamic pressure of droplet, i.e., $p = C\rho w_0^2$.
4) The contact pressure at the interface between splat and substrate in the region where flattening degree reaches to 1.5-2 is comparable to that resulting from explosive evaporation of surface adsorbed water. Beyond the region where the flattening degree is larger than 2, the contact pressure is not high enough to overcome other turbulent upward forces such as evaporated gas induced force to maintain a good contact between the droplet and substrate. It can be suggested that the reduced contact pres-

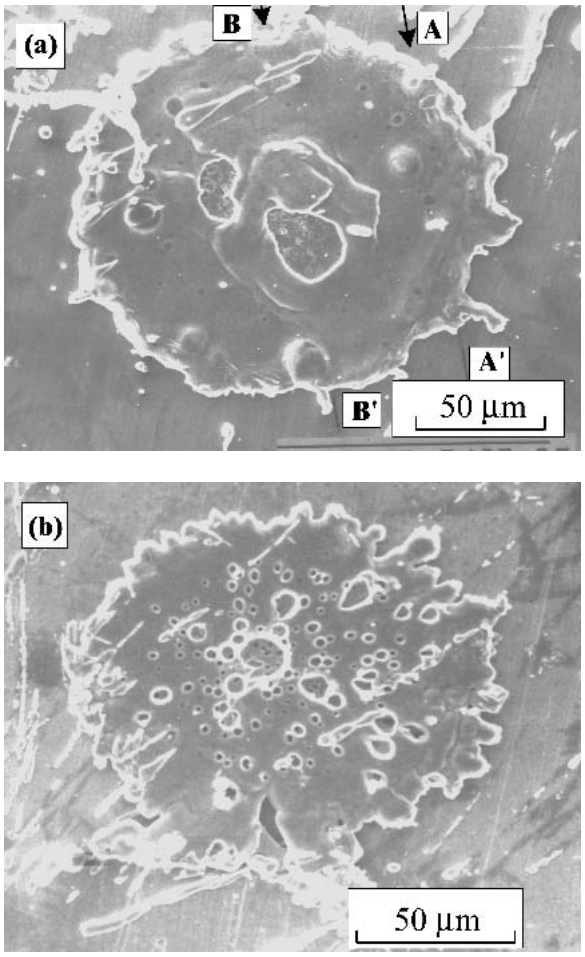

Fig. 7 Typical morphology of reduced Cu splat on stainless steel substrate surface (a) and Mo splat on Mo substrate surface (b)

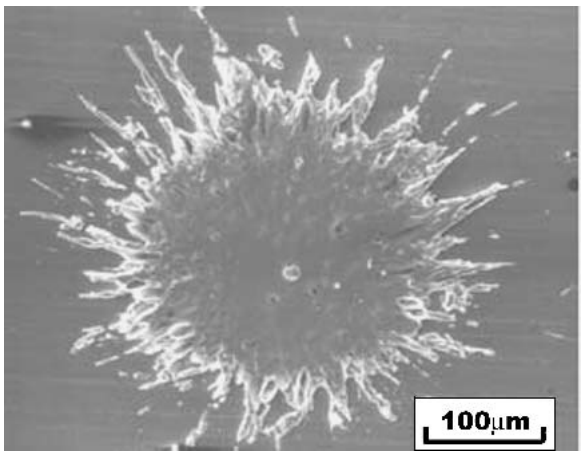

Fig. 8 Typical morphology of relatively complete disk-like splat deposited at a low plasma power (16kW).

sure at the late stage of spreading and disturbance by the evaporation-induced pressure resulting from rapid heating of the surface adsorbents by flattening droplet may contribute significantly to the splashing of the flattening droplet and the formation of a reduced disk-like splat.

Acknowledgment

The present work was supported by the National Natural Science Foundation of China (Contract No. 59401013).

References

1. H. Jones: "Cooling, Freezing and Substrate Impact of Droplets Formed by Rotary Atomization," *J. Phys. D: Appl. Phy.*, 1971, *4*, pp. 1657-60.
2. C-J. Li, A. Ohmori, and Y. Harada: "Experimental Investigation of the Morphologies of Plasma Sprayed Copper Splats," in *Thermal Spraying: Current Status and Future Trends*, A. Ohmori, ed., Japan High Temperature Society, Osaka University, Osaka, Japan, 1995, pp. 333-39.
3. C-J. Li, J-L. Li, W-B. Wang, A. Ohmori, and K. Tani: "Effect of Particle Substrate Materials Combinations on the Morphology of Plasma Sprayed Splats," in *Thermal Spray: Meeting the Challenges of the 21st Century*, C. Coddet, ed., ASM International, Materials Park, OH, 1998, pp. 481-88.
4. L. Bianchi, A. Grimaud, F. Blein, P. Lucchese, and P. Fauchais: "Comparison of Plasma-Sprayed Alumina Coatings by RF and DC Plasma Spraying," *J. Therm. Spray Technol*., 1995, *4*, pp. 59-66.
5. M. Fukumoto, S. Katoh, and I. Okane: "Splat Behavior of Plasma Sprayed Particles on Flat Substrate Surface" in *Thermal Spraying: Current Status and Future Trends*, A. Ohmori, ed., Japan High Temperature Society, Osaka University, Osaka, Japan, 1995, pp. 353-58.
6. C-J. Li, J-L. Li, and W-B. Wang: "The Effect of Substrate Preheating and Surface Organic Covering on Splat Formation," in *Thermal Spray: Meeting the Challenges of the 21st Century*, C. Coddet, ed., ASM International, Materials Park, OH, 1988, pp. 473-80
7. C-J. Li, A. Ohmori, and K. Tani: "The Morphology of Plasma-Sprayed Molybdenum Splats," in *Surface Modification Technology*, *Vol. X*, T.S. Sudarshan, K.A. Khor, and W. Reitz, ed., The Institute of Materials, London, 1997, pp. 934-45.
8. G. Trapaga, E.F. Matthys, J.J. Valencia, and J. Szekely: "Fluid Flow, Heat Transfer, and Solidification of Molten Metal Droplets Impacting on Substrates: Comparison of Numerical and Experimental Results," *Metall. Trans. B*, 1992, *23B,* pp. 701-18.
9. M. Bertagnolli, M. Marchese, and G. Jacucci: "Modeling of Particles Impacting on a Rigid Substrate Under Plasma Spraying Conditions," *J. Therm. Spray Technol.*, 1995, *4*, pp. 41-49.
10. H. Liu, E.J. Lavernia, and R.H. Rangel: "Numerical Simulation of Impingement of Molten Ti, Ni, and W Droplets on a Flat Substrate," *J. Therm. Spray Technol.*, 1993, *2*, pp. 369-78.
11. M. Bussmann, S.D. Aziz, S. Chandra, and J. Mostaghimi: "3D Modeling of Thermal Spray Droplet Splashing," in *Thermal Spray: Meeting the Challenges of the 21st Century*, C. Coddet, ed., ASM International, Materials Park, OH, 1998, pp. 413-18.
12. M. Vardelle, A. Vardelle, P. Fauchais, and C. Moreau: "Pyrometer System for Monitoring the Particle Impact on a Substrate During a Plasma Spray Process," *Meas. Sci. Technol.*, 1994, *5*, pp. 205-12.
13. J. Madejski: "Solidification of Droplets on a Cold Substrate," *Int. J. Heat Mass Transfer*, 1976, *19*, pp. 1009-13.
14. C-J. Li, J-L. Li., W-B. Wang, A-J. Fu, and A. Ohmori: "A Mechanism of the Splashing During Droplet Splatting in Thermal Spraying," in *Tagungsband Conference Proceedings*, E. Lugscheider and P.A. Kammer, ed., DVS German Welding Society, Germany, 1999, pp. 513-18.
15. X. Jiang, Y. Wan, H. Herman, and S. Sampath: "Role of Condensates and Adsorbates on Substrate Surface on Fragmentation of Impinging Molten Droplets During Thermal Spraying," *Thin Solid Films*, 2001, *385*, pp. 132-41.
16. M. Pasandideh-Fard, V. Pershin, I. Thomson, S. Chandra, and J. Mostaghimi: "Splat Shapes in a Thermal Spray Coating Process: Simulation and Experiments," *J. Therm. Spray Technol.*, 2002, *11,* pp. 206-17.
17. G. Montavon, Z.G. Feng, C. Coddet, Z.Q. Feng, and M. Domaszewski: "Influence of the Spray Parameters on the Transient Pressure Within a Molten Particle Impacting onto a Flat Substrate," in *Thermal Spray: A*

United Forum for Scientific and Technological Advances, C.C. Berndt, ed., ASM Internationals, Materials Park, OH, 1997, pp. 627-33.
18. H.I. Rosten and D.B. Spalding: Shareware PHOENICS Beginner's Guide: CHAM Report Number TR100, Concentration Heat and Momentum Ltd., London, UK, 1987.
19. A.A. Amsden and H.F. Harlow: "The SMAC Method: A Numerical Technique for Calculating Incompressible Fluid Flows," Los Alamos Scientific Laboratory Report, LA-4370, Los Alamos, NM, 1970.
20. C-J. Li and J-L. Li: "Numerical Simulations of Droplet Flattening in Plasma Spraying," *Aeronautical Manufacturing Technol.*, 1999, *5*, pp. 57-59 (in Chinese).
21. C-J. Li, H-L. Liao, P. Gougeon, G. Montavon, and C.Coddet: "Effect of Reynolds Number of Spray Particle on the Flattening Degree," in *Proceedings of 4th ITSC*, C. Moreau, ed., Orlando, ASM International, Materials Park, OH, 2003, pp. 875-82.
22. T.E. Faber: "*Fluid Dynamics for Physicists*," Cambridge University Press, Cambridge, UK, 1997.
23. O.G. Engel: "Waterdrop Collisions With Solid Surfaces," *J. Res. National Bureau of Standards*, 1955, *54*, pp. 281-98.
24. E. Honegger: "Tests on Erosion Caused by Jets," *Brow Boveri Rev*., 1927, *14*, p. 95.
25. J.E. Field: "ELSI Conference: Invited Lecture, Liquid Impact: Theory, Experiment, Applications," *Wear*, 1999, *233-235*, pp. 1-12.
26. P.A. Engel: "*Impact Wear of Materials*," Elsevier Scientific Publishing Company, Amsterdam, The Netherlands, 1976.
27. F.P. Bowden and D. Tabor: *The Friction and Lubrication of Solids*, Part II, The University Press, Oxford, London, UK, 1964.
28. R. McPherson and B.V. Shafer: "Interlamellar Contact Within Plasma-Sprayed Coatings," *Thin Solid Films*, 1982, *97*, pp. 201-04.
29. A. Ohmori and C-J. Li: "Quantitative Characterization of the Structure of Plasma Sprayed Al_2O_3 Coatings by Using Copper Electroplating," *Thin Solid Films*, 1991, *201*, pp. 241-52.
30. C-J. Li and A. Ohmori: "Relationship Between the Microstructure and Properties of Thermally Sprayed Deposits," *J. Therm. Spray Technol*., 2002, *11*, pp. 365-74.
31. C-J. Li, J-L. Li, and W-B. Wang: "Experimental Investigation of the Morphology of Plasma Sprayed Nickel Splats," in *Proceedings of C-MRS (China Materials Research Society) and MRS-K (Materials Research Society of Korea) Joint Symposium*, Beijing, China, K. Zhou, L. Wen, and H.M. Jang, ed., Chemical Industrial Publishing House, Beijing, 1996, pp. 768-71.
32. S. Glod, D. Poulikakos, Z. Zhao, and G. Yadigarogglu: "An Investigation of Microscale Explosive Evaporization of Water on an Ultrathin Pt Wire," *Inter. J. Heat and Mass Transfer*, 2002, *45*, pp. 367-79.
33. C. Moreau, P. Gougeon, and M. Lamontagne: "Influence of Substrate Preparation on the Flattening and Cooling of Plasma-Sprayed Particles," *J. Therm. Spray Technol*., 1995, *4*, pp. 25-33.
34. H.K. Park, D. Kim, and C.P. Grigoropoulos: "Pressure Generation and Measurement in the Rapid Vaporization of Water on a Pulsed-Laser-Heated Surface," *J. Appl. Phys,* 1996, *80,* pp. 4072-81.